Ultrasound-Assisted Synthesis of SnS_2 Quantum Dots Using Acetone as Solvent

Grzegorz Matyszczak *, Krzysztof Krawczyk, Albert Yedzikhanau, Cezariusz Jastrzębski, Piotr Dluzewski, Aleksandra Fidler, Tomasz Płociński, Krystyna Ławniczak-Jabłońska, Anna Wolska, Aleksandra Drzewiecka-Antonik

Posted Date: 26 November 2024

doi: 10.20944/preprints202411.1987.v1

Keywords: sonochemistry; quantum dots; tin(IV) sulphide

Article

Ultrasound-Assisted Synthesis of SnS_2 Quantum Dots Using Acetone as Solvent

Grzegorz Matyszczak [1,*], Krzysztof Krawczyk [1], Albert Yedzikhanau [1], Cezariusz Jastrzębski [2], Piotr Dłużewski [3], Aleksandra Fidler [3], Tomasz Płociński [4], Krystyna Lawniczak-Jablonska [3], Anna Wolska [3] and Aleksandra Drzewiecka-Antosik [3]

[1] Faculty of Chemistry, Warsaw University of Technology
[2] Faculty of Physics, Warsaw University of Technology
[3] Institute of Physics, Polish Academy of Sciences
[4] Faculty of Materials Science and Engineering, Warsaw University of Technology
* Correspondence: grzegorz.matyszczak@pw.edu.pl

Abstract: A sonochemical synthesis of SnS_2 quantum dots using acetone as a solvent is investigated. Two different tin sources ($SnCl_2 \cdot 2H_2O$ or $SnCl_4 \cdot 5H_2O$) as well as two different sulphur sources (thioacetamide or $Na_2S_2O_3$) were applied. The sonication time was also varied between 60 and 120 minutes. Resulting products of syntheses were characterized with the following techniques: powder X-ray diffraction, electron microscopy (SEM and HR-TEM), Raman and FT-IR spectroscopies, the Tauc method, and X-ray photoelectron spectroscopy. Obtained SnS_2 nanostructures were in the form of quantum dots in the case of synthesis lasting 60 minutes (size of crystallites in the range of 3.5 – 7 nm) and in the form of elongated nanorods of length c.a. 25-30 nm and width of 5-6 nm in the case of synthesis lasting 120 minutes. XPS analyses revealed that the surface of the obtained products contained significant amount of tin at the second oxidation state (i. e. SnS). The quantum dots produced in the synthesis lasting 60 minutes showed value of energy bandgap of 2.7 eV indicating potential applications in photocatalysis.

Keywords: sonochemistry; quantum dots; tin(IV) sulphide

1. Introduction

Tin chalcogenides are a well-known group of inorganic chemical compounds. Their specific structural properties allow for formation of very interesting, possible new mixed-valence tin chalcogenides [1]. For example, tin together with sulfur forms two basic tin sulfides (SnS and SnS_2), however they may be 'mixed' to form other two known tin sulfides (Sn_2S_3 and Sn_3S_4) [1–3]. These compounds compose of SnS and SnS_2 "units" mixed in certain proportions (e.g. 1 : 1 and 2 : 1 for Sn_2S_3 and Sn_3S_4 respectively) [2–4]. This fact contributes to rich and interesting chemistry of tin chalcogenides [5].

Tin chalcogenides, due to their wide properties, are interesting also from the perspective of materials science. Tin(II) sulfide is a semiconductor with optical energy band gap lying typically in the range of 1.1 – 1.5 eV [6]. It is also characterized by p-type conductivity and relatively large optical absorption coefficient. Thus SnS is an attractive material for utilization in fields such as photonics, photovoltaics, and optoelectronics [7,8]. Other two tin sulfides, Sn_2S_3 and SnS_2, have conductivity of n-type which is caused by sulfur vacancy related to the Sn(IV) oxidation state [6].

Wide applications of tin sulphides often require preparation of this compounds in the form of nanostructures. Among methods that have been used to prepare tin(II) and tin(IV) sulphide nanostructures one can mention: solvothermal (including hydrothermal) routes, the hot injection method, polyol methods, and precipitation from aqueous solutions [9–16]. However, these methods typically involve usage of toxic high-boiling solvents and/or toxic reagents. A promising alternative for these methods is the sonochemical synthesis which meets the criteria of the so-called "Green Chemistry" [17]. The sonochemical synthesis was successfully used for the preparation of inorganic

 doi:10.20944/preprints202411.1987.v1

nanostructures of simple (e.g. ZnS, CdS) and complex (e.g. Cu_3BiS_3, $CuInS_2$, Cu_2ZnSnS_4) inorganic compounds [18–22]. By the manipulation of the parameters of the sonochemical synthesis one can achieve many morphologies and sizes of products, however the control of product may be additionally enhanced by merging sonochemical and electrochemical syntheses [23–26].

Tin sulphides were prepared via the ultrasound-assisted synthesis many times. Nanoparticles of SnS were synthesized using direct sonication and reagents such as $SnCl_2$, $Na_2S_2O_3$ or Na_2S, and CH_3COONH_4 in unknown solvent [27–29]. Indirect sonication was also used in the sonochemical synthesis of SnS resulting in nanoparticles of 7 nm in the mean size, however also in unknown solvent [30]. Using a mixture of ethanol and ionic liquid (1-buthyl-3methylimidazole tetrafluoroborane), and thioacetamide as a source of sulphur allowed for the synthesis of SnS with particles of sizes in range from 50 to 700 nm [31]. On the other hand, starting from the same reagents but using ethylene glycol mixed with a amine (ethanolamine, diethanolamine or triethanolamine) it was possible to achieve SnS nanoparticles with size in range of 4 to 15 nm [32]. There are fewer reports on the sonochemical synthesis of SnS_2 in comparison with SnS. However, SnS_2 nanoparticles of sizes in range 24 – 30 nm were prepared in aqueous solutions of $SnCl_4$ and thioacetamide with optional addition of concentrated hydrochloric acid [33–35]. Finally, quantum dots of both tin sulfides, with sizes varying from 1.5 to 10 nm for SnS_2 and from 3 to 8 nm for SnS, were sonochemically obtained using the most technologically desirable solvent, which is water [36]. Despite described approaches for the sonochemical synthesis of SnS and SnS_2 (preferably in the form of quantum dots), the influence of utilized solvent on the product is still unclear and more studies (using other solvents) need to be conducted.

This study presents the investigation of possible application of acetone as a solvent in the sonochemical synthesis of SnS and SnS_2 quantum dots. Following starting reagents were used: $SnCl_2$ or $SnCl_4$ (as a source of tin) and thioacetamide or sodium thiosulfate (as a source of sulphur). Resulting products of syntheses were isolated, purified and subjected for investigations with following techniques: powder X-ray diffraction, Raman and FT-IR spectroscopies, UV-Vis spectrophotometry (estimation of energy bandgap with the Tauc method), electron microscopy (SEM and HR-TEM), and X-ray photoelectron spectroscopy (XPS).

2. Materials and Methods

2.1. Materials and Reagents

All chemicals used in this study were pure for analysis (producer: POCH – Polskie Odczynniki Chemiczne). For sonochemical syntheses, $SnCl_2{\cdot}2H_2O$, $SnCl_4{\cdot}5H_2O$, $Na_2S_2O_3$, and thioacetamide (TAA) were used as reagents. Acetone was used as a solvent in the syntheses and ethanol was used for the purification of prepared suspensions.

2.2. Sonochemical Syntheses

The sonochemical syntheses were conducted in conical flasks of 50 ml volume in an ultrasonic cleaner (PS 10A) generating an ultrasound of 40 kHz frequency with nominal power of ultrasounds 60 W. The acoustic power determined by the calorimetric method was 27.9 W/L.

20 ml of acetone was measured with a graduated pipette and placed in a flask. Weighed reagents (see Table 1 for detailed information on amounts) were placed in the solvent in the conical flask and the mixture then was stirred magnetically for 20 minutes. Next, the flasks were closed with glass stoppers and placed in the ultrasonic cleaner so the level of liquid in cleaner was the same as the level of liquid in the flasks. The duration of sonication was 60 or 120 minutes.

Immediately after the reaction the conical flasks were opened and kept under laboratory hood for a c.a. 1 hour to remove the potentially toxic gases produced during the reaction. After that, the produced powders were purified by subsequent centrifugations according to the following procedure: first, the reaction mixture was centrifuged and the supernatant was removed; next, the sediment was suspended in fresh ethanol (10 ml) in the ultrasonic cleaner for 10 minutes; then the obtained suspension has been centrifuged, supernatant was removed and the sediment was

 doi:10.20944/preprints202411.1987.v1

suspended in fresh portion of ethanol (10 ml) in the ultrasonic cleaner for 10 minutes (this point was repeated additionally 2 times). Such a procedure resulted in a suspension in ethanol of the synthesized powders.

Table 1. Summary of experimental conditions of conducted sonochemical syntheses.

No. (and sample name if available)	Tin source	Amount of tin source [mg]	Sulphur source	Amount of sulphur [mg]	Sonication time source[min]	Result of synthesis
1	$SnCl_4 \cdot 5H_2O$	702	Thioacetamide	376	60	Clear, yellow solution (no precipitate after centrifugation)
2	$SnCl_4 \cdot 5H_2O$	702	Thioacetamide	376	120	Yellow suspension (no precipitate after centrifugation)
3 (A35)	$SnCl_2 \cdot 2H_2O$	452	Thioacetamide	376	60	Yellow precipitate
4 (A36)	$SnCl_2 \cdot 2H_2O$	452	Thioacetamide	376	120	Yellow precipitate
5	$SnCl_4 \cdot 5H_2O$	702	$Na_2S_2O_3$	1242	60	Reaction mixture unchanged
6	$SnCl_4 \cdot 5H_2O$	702	$Na_2S_2O_3$	1242	120	Reaction mixture unchanged
7	$SnCl_2 \cdot 2H_2O$	452	$Na_2S_2O_3$	1242	60	Reaction mixture unchanged
8	$SnCl_2 \cdot 2H_2O$	452	$Na_2S_2O_3$	1242	120	Reaction mixture unchanged.

2.3. UV-Vis Spectrophotometry

The UV-Vis spectra of diluted transparent suspensions in ethanol of synthesized powders were recorded within the wavelength range of 380-1000 nm using a spectrophotometer Model UV1600 (AOE Instruments). The collected spectra were subsequently used to perform analyses based on the Tauc method.

2.4. SEM Investigations

SEM observations were carried out on the Filed Emission Scanning Electron Microscope (FE-SEM) made by Hitachi High Technologies company, model SU8000. The images were taken with upper detector which is semi in-lens type detector, and provide best resolution. The magnification range of 20 000x up to 100 000x at 5keV and short working distance was used to determine the fine structure of particles.

2.5. Raman Spectroscopy

Raman measurements were conducted using an Aramis spectrometer of Horiba Jobin Ivon in backscattering geometry. The 633 nm line of the He-Ne–ion laser was used as the excitation. Raman spectra were collected using a 2400 l/mm diffraction grating and thermoelectric-cooled Synapse CCD

 doi:10.20944/preprints202411.1987.v1

at room temperature and under normal conditions. The spectral resolution of the measured spectra in this configuration was about 1cm^{-1}. A low-power laser beam was used to avoid thermal effects.

2.6. FTIR Spectroscopy

The Fourier-transform infrared spectroscopy measurements were conducted using NICOLET 6700 FT-IR spectrometer. Synthesized, dry powders were grounded with KBr and formed as pellets.

2.7. HR-TEM Investigations

One drop of the powder suspended in ethanol was deposited on a standard TEM copper grid coated with an amorphous carbon film. The grid was dried afterwards and then used for the TEM investigation.

Investigations were conducted with the use of FEI Titan Cubed 80-300 TEM operating at 300 kV. The overview images were registered in bright-field TEM mode for magnifications ranging from 27.000x to 89.000x. For the purpose of high-resolution imaging magnifications from 380.000x - 420.000x range were used. In both cases, the images were obtained with the Gatan BM-Ultrascan CCD camera.

2.8. XPS Investigations

The suspensions of samples were dripped on Cu conductive tape and left to dry in laboratory fume cupboard. The procedure was repeated until a visible sample layer was obtained then samples were introduced to the spectrometer. X-ray photoelectron spectra (XPS) were recorded by Prevac set-up equipped with high intensity monochromatic X-ray Al Kα (1486.69 eV) source Scienta MX 650 (set at 300 W), Scienta R4000 hemispherical analyser, and charge neutralization. The narrow scans were acquired with pass energy 200 eV and the step 0.2 eV. The full width at half maximum (FWHM) for the Au 4f 7/2 line measured at the same experimental condition was equal to 0.6 eV. The energy scale was calibrated setting the C 1 s line at the position 285.0 eV. Spectra were analysed using the commercial CASA XPS software package (Casa Software Ltd, version 2.3.17) with Tougaard background and a GL (30) line shape (70 % Gaussian, 30 % Lorentzian). The wide spectra were registered with pass energy 500 eV and the step 0.5 eV.

3. Results and Discussion

According to data presented in Table 1, only two experimental setups led to the formation of precipitates that were possible to separate by the centrifugation. Such yellow precipitates had a color characteristic for tin(IV) sulphide (SnS_2) which can't be matched with any other known tin sulphide (SnS – dark brown, Sn_2S_3 – brown). Yellow precipitates were obtained using $SnCl_2{\cdot}2H_2O$ as the tin source and thioacetamide as the sulphur source, with no relation to the sonication time. Using the same sulphur source but with $SnCl_4{\cdot}5H_2O$ as the tin source the reaction mixture turned to yellow color after the sonication but no precipitate was possible to separate by the centrifugation. The opacification was greater in the case of longer sonication time. The resulting yellow color without separable precipitate indicates the formation of ultrasmall nanoparticles of SnS_2 with probably greater yield in the 120 minutes long synthesis. On the other hand, in the case of usage of $Na_2S_2O_3$ as the sulphur source, the reaction mixtures remained unchanged even after 120 minutes of sonication which indicates no reaction, at least toward the formation of tin sulphides.

The results of the X-ray powder diffraction investigations conducted on the two yellow precipitates suggest the presence of tin(IV) sulphide in the nanocrystalline form. This is indicated by the broadening of the reflexes in the powder diffractogram, as well as by the absence of the large and wide peak in the range of angle from 10 to 15 ° (see Figure 1).

 doi:10.20944/preprints202411.1987.v1

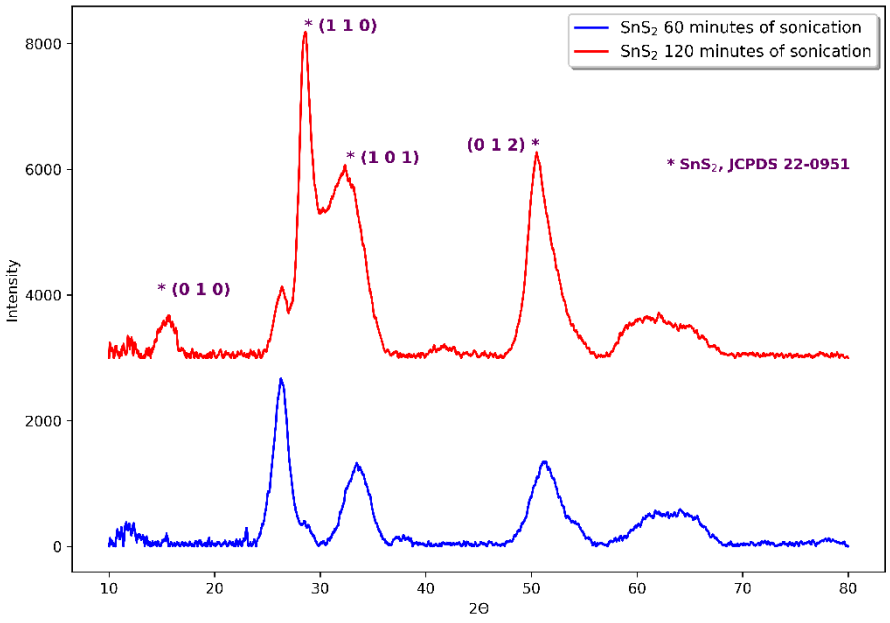

Figure 1. X-ray powder diffractograms of yellow precipitates obtained in the sonochemical syntheses performed in acetone using $SnCl_2 \cdot 2H_2O$ and thioacetamide as reagents and with sonication time 60 minutes (bottom curve) and 120 minutes (upper curve).

Raman studies confirmed the formation of SnS_2 nanograins in the sonochemical synthesis process. There were no precipitations of another phase. The Eg and A1g symmetry peaks indicate a trigonal crystal structure of SnS_2 with a 2H polytype. This is evidenced mainly by a clear peak of A_{1g} for about 315 cm^{-1} (Figure 2) [37,38]. The intensity of the E_g peak at about 205 cm^{-1} is very low and hardly observed.

A slight shift of this peak of about 0.5 cm^{-1} towards higher frequencies in the case of A35 sample compared to the A36 sample was observed. This may be attributed to small amounts of polytypes different from 2H in the A35 sample [39]. Some asymmetry of the peak was observed for both types of samples. Such asymmetry may be caused by phonon-free carriers interaction or is due to phonon constraints in nanostructures [40]. In the case of SnS_2, this broadening may result also from the disorder activation of forbidden phonons with A_{2u} symmetry [41].

The asymmetry of the A_g peak is greater in the case of A35 samples. At the same time, a much higher luminescence background is observed for these samples. Hence, it can be concluded that the broadening of the A_g peak results from a higher concentration of defects and activation of phonons normally forbidden by the selection rules.

 doi:10.20944/preprints202411.1987.v1

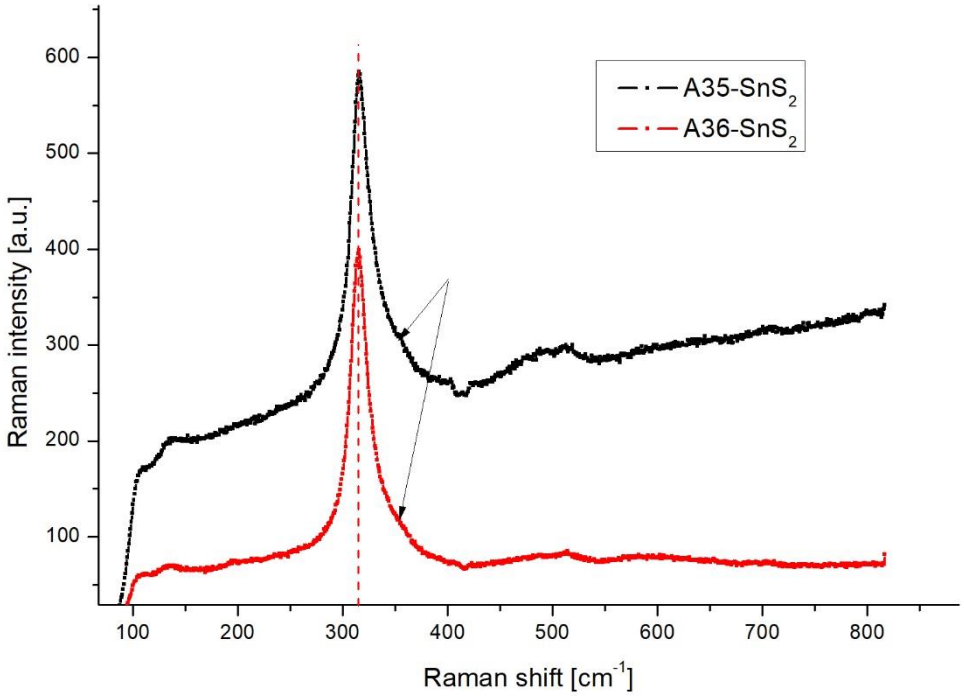

Figure 2. Typical Raman spectra of samples A35 and A36. A vertical dashed line was placed for 315 cm^{-1}. Arrows indicate asymmetry of the A_{1g} peak.

Additional FT-IR spectroscopy investigations were conducted to confirm the presence of tin(IV) sulphide (Figure 3). In both yellow precipitates a Sn-S bonds are presented (region of 1000 – 1300 cm^{-1}). The FT-IR spectra show the occurrence of trace amounts of solvent used in purification (C_2H_5OH) as indicated by peaks corresponding to C-C and C-H bonds, and –OH groups (1400, 1600, and 3000-3500 cm^{-1}). The bands related to Sn-S bond are similar in both samples of SnS_2 what is in line with the XRD and Raman results.

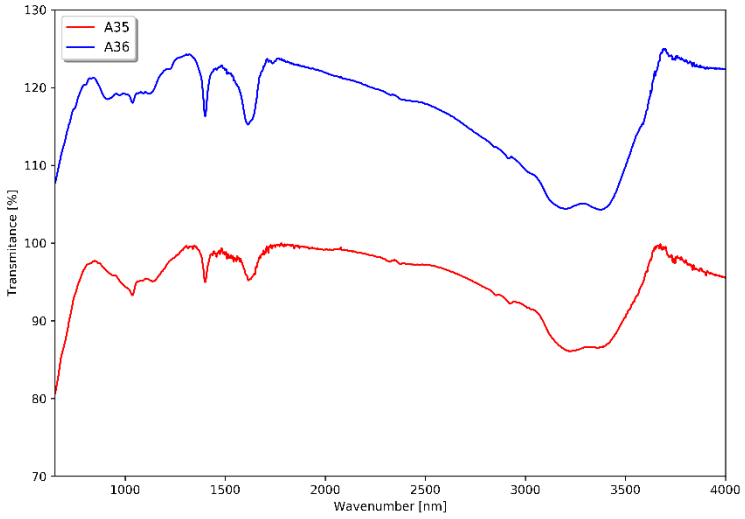

Figure 3. FT-IR spectra of samples A35 and A36.

The morphology of the dried yellow precipitates was investigated by the scanning electron miscroscopy (SEM) observations. The dried product of reaction that durated 60 minutes formed submicron agglomerates (Figure 4a) made of nanometric particles (Figure 4b). On the other hand, the dried product of 120 minutes long reaction formed submicron particles with interesting, flower-like

 doi:10.20944/preprints202411.1987.v1

morphology (Figure 4c). Observations in higher magnitude revealed that the flower-like particles are made of elongated and narrow nanostructures (Figure 4d). The EDX elemental analyses confirmed the presence of desired elements (Sn and S) in the obtained powders, however with deviations from ideal atomic ratio of Sn to S which in bulk SnS_2 is 1 : 2. For the powder obtained in the 60 minutes long synthesis, the Sn : S ratio is 1.75 : 1, while for the powder obtained in the 120 minutes long synthesis, the Sn : S ratio is 0.73 : 1. The difference from the ideal ratio may be likely caused by the formation of nanoparticles in the syntheses, however it may be seen that with longer sonication time the Sn : S ratio changed its value toward the ideal one.

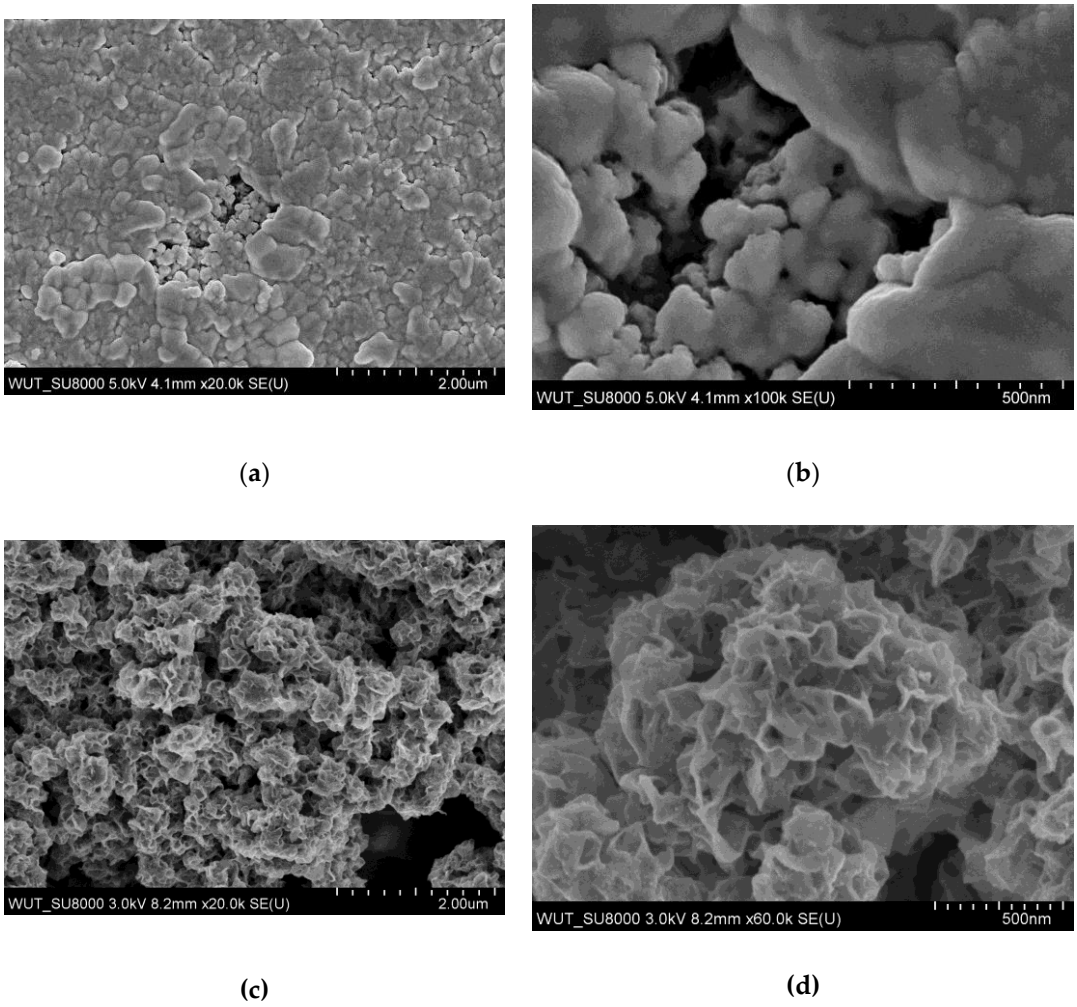

Figure 4. SEM images of dried products of syntheses with duration: a, b) 60 minutes; c, d) 120 minutes.

Observations made by the HR-TEM technique proved the presence of nanocrystallites in the prepared samples of SnS_2 (Figure 5). In the product of synthesis lasting 60 minutes, nanocrystallites with sizes in range from 3.5 to 7.5 nm were confirmed (Figure 5a). Elongated and narrow nanostructures were present in the sample obtained by 120 minutes long sonication (Figure 5b).

Preprints.org (www.preprints.org) | NOT PEER-REVIEWED | Posted: 26 November 2024 doi:10.20944/preprints202411.1987.v1

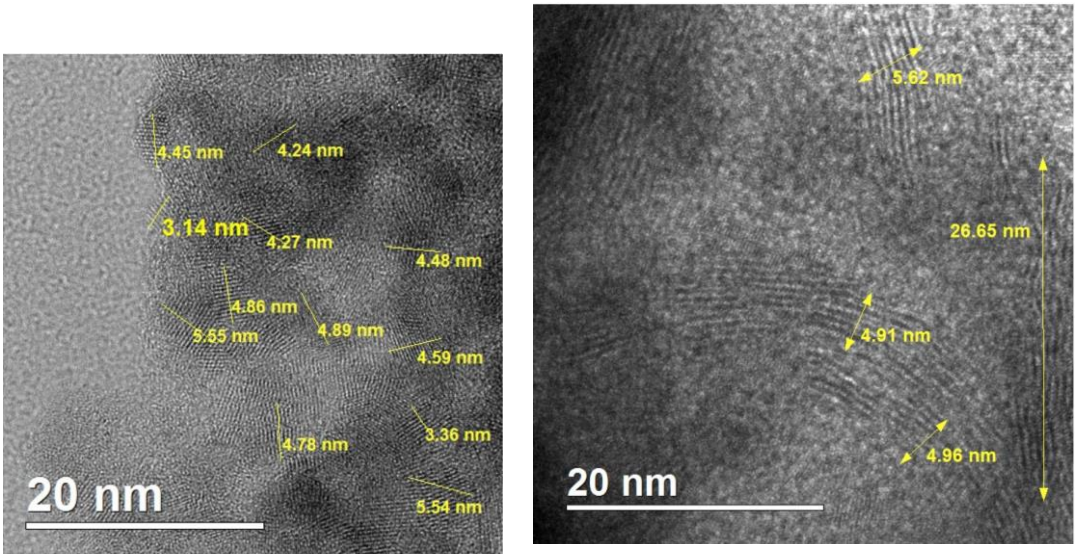

(**a**) (**b**)

Figure 5. HR-TEM images of the products of syntheses with duration: a) 60 minutes, b) 120 minutes.

Further observations with HR-TEM technique and analyses based on their Fourier transforms confirm that nanocrystallites have structure typical for SnS_2 (Berndtite structure – see Figure 6).

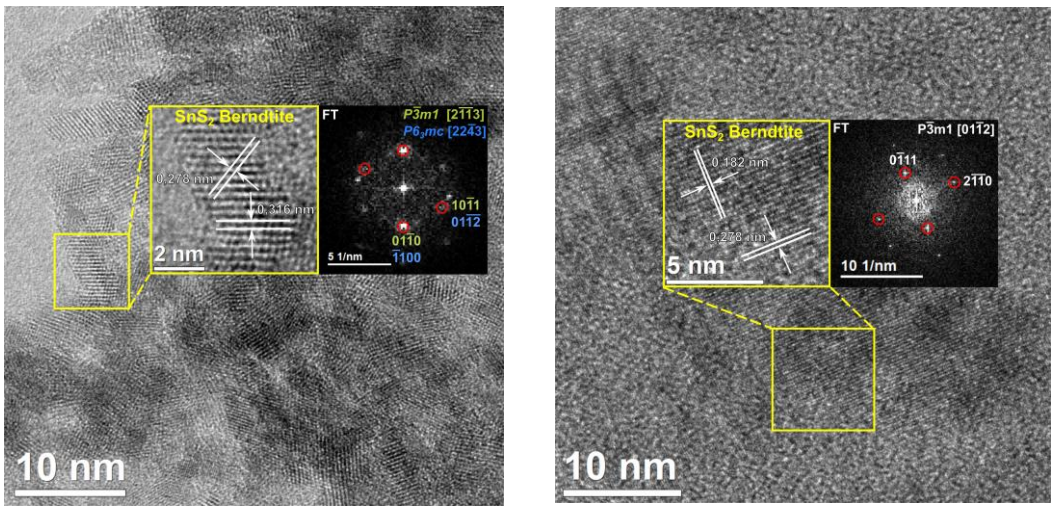

(**a**) (**b**)

Figure 6. HR-TEM images, together with Fourier transforms, of dried products of syntheses with duration: a) 60 minutes; b) 120 minutes. (Red circles indicate spots corresponding to the structure of the analyzed nanocrystal, other spots come from neighboring ones).

The results of the X-ray photoelectron spectroscopy investigations are presented in Tables 2 and 3. Like the results of the EDX elemental analysis, they indicate that the Sn : S ratio evolves toward ideal ratio of value 1 : 2 with longer synthesis times. However, it turns out that on the surface of both samples the main component is not SnS_2, but SnS. Additionally, the fraction of SnS_2 on the surface of product decreases with increasing sonication time. Quite high values of FWHM and slightly changed binding energy of the fitting curves indicated a large disorder in the chemical structure of the formed

 doi:10.20944/preprints202411.1987.v1

nanoparticles, therefore, we cannot exclude the possibility of the formation of other compounds such as e.g. Sn_2S_3 or Sn_3S_4.

Table 2. Results of the XPS elemental composition (at %) of tested samples from high and low (survey) resolution spectra.

Sonication time [min]	Spectrum resolution	Sn	S	C	O	S:Sn
60	High	14.7	12.5	17.5	55.3	0.85
60	Low	14.3	15.4	20.0	50.3	1.1
120	High	7.2	9.5	70.2	13.1	1.3
120	Low	0.74	1.6	77.5	20.2	2.2

Table 3. The binding energy (eV); percentage of given fraction, and full width at half maximum (eV) (FWHM) for chemical components in analyzed samples. FWHM indicates the level of chemical order in formed compounds.

Sonication time [min]	BE of S in SnS	FWHM	BE of S in SnS_2	FWHM	BE of Sn(II) in SnS	FWHM	BE of Sn(IV) in SnS_2	FWHM
60	161.9; 74.1%	0.9	162.6: 25.9%	1.3	486.6; 88.2%	1.1	487.3; 11.9%	1.5
120	161.3; 94.8%	1.0	162.6; 5.2%	1.1	486.5; 94.8%	1.2	487.6; 5.2%	0.9

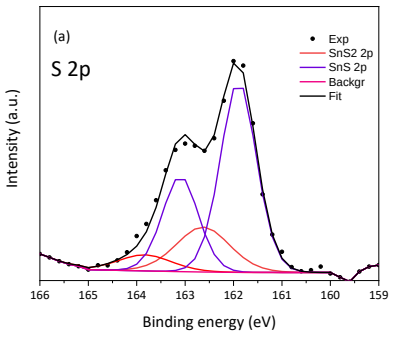

(**a**)

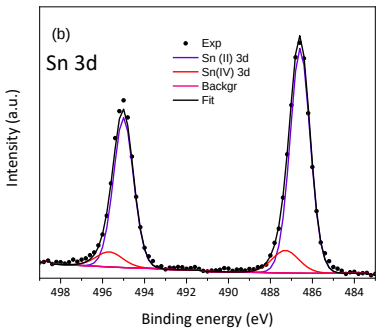

(**b**)

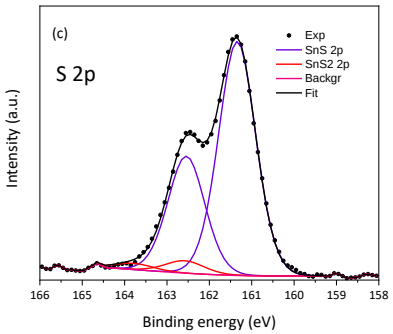

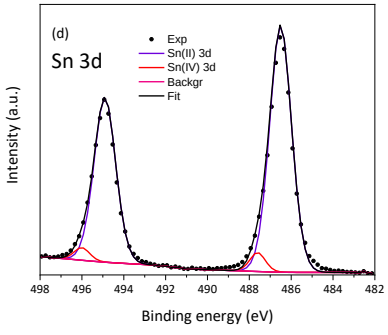

 doi:10.20944/preprints202411.1987.v1

(c) **(d)**

Figure 7. XPS spectra of S 2p (a and c) and Sn 3d (b and d) of sonochemically synthesized SnS_2 quantum dots: a, b) 60 minutes long synthesis; c, d) 120 minutes long synthesis.

The analyses performed basing on the Tauc approximation revealed that the product of synthesis lasting 60 minutes has value of energy bandgap for direct transition of 2.7 eV (see Figure 8a for relevant Tauc plot). Such a value is slightly greater than the value corresponding to the bulk SnS_2 which is c.a. 2.4 eV [42]. The inrease in the energy bandgap is likely caused by the quantum confinement effect. On the other hand, the product of synthesis lasting 120 minutes is characterized by energy bandgap of value 1.5 eV for direct transition (see Figure 8b) exhibiting a significant difference in comparison with the bulk SnS_2. Such a result may suggest the presence of other phases (SnS, Sn_2S_3, Sn_3S_4) in the prepared powder of SnS_2. The values of optical energy bandgaps suggest possible applications of prepared quantum dots in the field of photocatalysis (product of synthesis lasting 60 minutes; relatively high value of 2.7 eV) and photovoltaics (product of synthesis lasting 120 minutes; value 1.5 eV lying in the so-called Schockley-Queisser limit [43]).

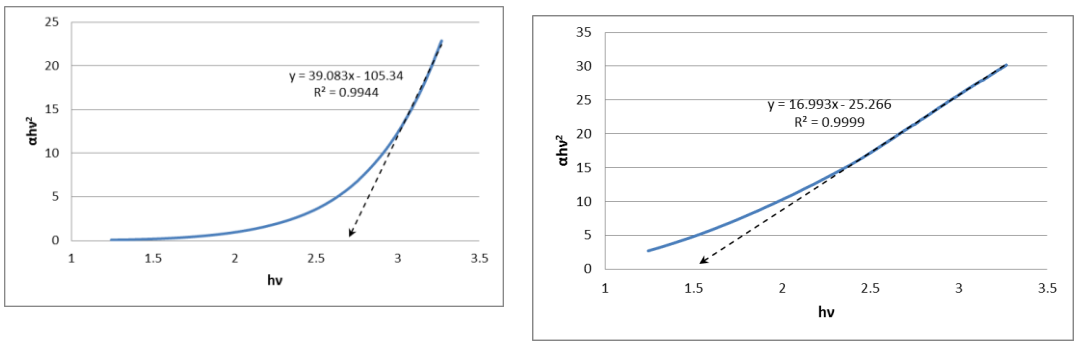

(a) **(b)**

Figure 8. The Tauc plots of sonochemically synthesized SnS_2 quantum dots: a) 60 minutes long synthesis; b) 120 minutes long synthesis.

4. Conclusions

We present a procedure for the sonochemical synthesis of SnS_2 quantum dots using, for the first time, acetone as a solvent. Different tin and sulphur sources were investigated and it turned out that SnS_2 nanostructures may be obtained using $SnCl_2{\cdot}2H_2O$ and thioacetamide. Obtained SnS_2 nanostructures were in the form of quantum dots in the case of synthesis lasting 60 minutes (size of crystallites in the range of 3.5 – 7 nm) and in the form of elongated nanorods of length c.a. 25-30 nm and width of 5-6 nm in the case of synthesis lasting 120 minutes. XPS analyses revealed that on the surface the obtained products contained significant amount of tin on the second oxidation state (i. e. SnS). The estimated values of energy bandgaps suggest potential applications of synthesized quantum dots in the field of photocatalysis (product of 60 minutes long synthesis – 2.7 eV) and photovoltaics (product of 120 minutes long synthesis – 1.5 eV).

Author Contributions: Grzegorz Matyszczak: Conceptualization, Methodology, Supervision, Writing- Original draft preparation, Investigation, Writing- Reviewing and Editing, Visualization, Formal analysis. Tomasz Płociński: Visualization, Investigation, Formal analysis. Piotr Dłużewski: Visualization, Investigation, Formal analysis. Aleksandra Fidler: Visualization, Investigation, Formal analysis. Cezariusz Jastrzębski: Visualization, Investigation, Formal analysis, Writing- Original draft preparation. Krystyna Ławniczak-Jabłońska: Visualization, Investigation, Formal analysis of XPS. Anna Wolska : XPS Investigation. Aleksandra Drzewiecka-Antonik: XPS Investigation. Albert Yedzikhanau: Investigation. Krzysztof Krawczyk: Supervision. All authors have read and agreed to the published version of the manuscript.

Funding: Research was funded by Warsaw University of Technology within the Excellence Initiative: Research University (IDUB) programme.

Data Availability Statement: Dataset available on request from the authors.

Acknowledgments: We would like to thank Mrs. Boguslawa Adamczyk-Cieslak for experimental support.

Conflicts of Interest: The authors declare no conflict of interest.

References

1. Burton, L. A.; Colombara, D.; Abellon, R. D.; Grozema, F. C.; Peter, L. M.; Savenije, T. J.; Dennler, G.; Walsh, A. Synthesis, Characterization, and Electronic Structure of Single-Crystal SnS, Sn_2S_3, and SnS_2. *Chem. Mater.* **2013**, *25*, 4908-4916. http://dx.doi.org/10.1021/cm403046m
2. Yuan, C.; Hou, L.; Yang, L.; Fan, C.; Li, D.; Li, J.; Shen, L.; Zhang, F.; Zhang, X. Interface-hydrothermal synthesis of Sn_3S_4/graphene sheet composites and their application in electrochemical capacitors. *Mater. Lett.* **2011**, *65*, 374-377. https://doi.org/10.1016/j.matlet.2010.10.045
3. Li, J.; Han, L.; Li, Y.; Li, J.; Zhu, G.; Zhang, X.; Lu, T.; Pan, L. MXene-decorated SnS_2/Sn_3S_4 hybrid as anode material for high-rate lithium-ion batteries. *Chem. Eng. J.* **2020**, *380*, 122590. https://doi.org/10.1016/j.cej.2019.122590
4. Wang, X.; Liu, Z.; Zhao, X.-G.; Lv, J.; Biswas, K.; Zhang, L. Computational Design of Mixed-Valence Tin Sulfides as Solar Absorbers. *ACS Appl. Mater. Interfaces* **2019**, *11*, 24867-24875. https://doi.org/10.1021/acsami.9b01223
5. Greenwood, N. N.; Earnshaw, A. *The Chemistry of the Elements.* Pergamon Press, 1984.
6. Whittles, T. J.; Burton, L. A.; Skelton, J. M.; Walsh, A.; Veal, T. D.; Dhanak, V. R. Band Alignments, Valence Bands, and Core Levels in the Tin Sulfides SnS, SnS_2, and Sn_2S_3: Experiment and Theory. *Chem. Mater.* **2016**, *28*, 3718-3726. https://doi.org/10.1021/acs.chemmater.6b00397
7. Lewis, D. J.; Kevin, P.; Bakr, O.; Muryn, C. A.; Malik, M. A.; O'Brien, P. Routes to tin chalcogenide materials as thin films or nanoparticles: a potentially important class of semiconductor for sustainable solar energy conversion. *Inorg. Chem. Front.* **2014**, *1*, 577-598. https://doi.org/10.1039/C4QI00059E
8. Reddy, N. K.; Devika, M.; Gopal, E. S. R. Review on Tin (II) Sulfide (SnS) Material: Synthesis, Properties, and Applications. *Crit Rev Solid State* **2015**, *40*, 359-398. https://doi.org/10.1080/10408436.2015.1053601
9. Zhu, H.; Yang, D.; Ji, Y.; Zhang, H.; Shen, X. Two-dimensional SnS nanosheets fabricated by a novel hydrothermal method. *J. Mater. Sci.* **2005**, *40*, 591-595. https://doi.org/ 10.1007/s10853-005-6293-x
10. An, C.; Tang, K.; Shen, G.; Wang, C.; Yang, Q.; Hai, B.; Qian, Y. Growth of belt-like SnS crystals from ethylenediamine solution. *J. Cryst. Growth* **2002**, *244*, 333-338. https://doi.org/10.1016/S0022-0248(02)01613-5
11. Hickey, S. G.; Waurisch, C.; Rellinghaus, B.; Eychmüller, A. Size and Shape Control of Colloidally Synthesized IV-VI Nanoparticulate Tin(II) Sulfide. *J. Am. Chem. Soc.* **2008**, *30*, 14978-14980. https://doi.org/10.1021/ja8048755
12. Liu, Y.; Hou, D.; Wang, G. Synthesis and characterization of SnS nanowires in cetyltrimethylammoniumbromide (CTAB) aqueous solution. *Chem. Phys. Lett.* **2003**, *379*, 67-73. https://doi.org/10.1016/j.cplett.2003.08.014
13. Shen, G.; Chen, D.; Tang, K.; Huang, L.; Qian, Y.; Zhou, G. Novel polyol route to nanoscale tin sulfides flaky crystallines. *Inorg. Chem. Commun.* **2003**, *6*, 178-180. https://doi.org/10.1016/S1387-7003(02)00716-5
14. Gajendiran, J.; Rajendran, V. Synthesis of SnS_2 nanoparticles by a surfactant-mediated hydrothermal method and their characterization. *Adv. Nat. Sci.: Nanosci. Nanotechnol.* **2011**, *2*, 015001. http://dx.doi.org/10.1088/2043-6262/2/1/015001
15. Xiao, H.; Zhang, Y. C. In air synthesis of SnS_2 nanoplates from tin, sulfur and ammonium choride powders. *Mater. Chem. Phys.* **2008**, *112*, 742-744. https://doi.org/10.1016/j.matchemphys.2008.07.119
16. Giberti, A.; Gaiardo, A.; Fabbri, B.; Gherardi, S.; Guidi, V.; Malagu, C.; Bellutti, P.; Zonta, G.; Casotti, D.; Cruciani, G. Tin(IV) sulfide nanorods as a new gas sensing material. *Sens Actuators B Chem* **2016**, *223*, 827-833. https://doi.org/10.1016/j.snb.2015.10.007
17. Okitsu, K.; Cavalieri, F. *Sonochemical Production of Nanomaterials, SpringerBriefs in Molecular Science: Ultrasound and Sonochemistry;* Springer Nature, 2018.
18. Liu, Y.; Xu, J.; Ni, Z.; Fang, G.; Tao, W. One-step sonochemical synthesis route towards kesterite Cu_2ZnSnS_4 nanoparticles. *J. Alloys Compd.* **2015**, *630*, 23-28. https://doi.org/10.1016/j.jallcom.2015.01.033
19. Gedanken, A. Using sonochemistry for the fabrication of nanomaterials. *Ultrason. Sonochem.* **2004**, *11*, 47-55. https://doi.org/10.1016/j.ultsonch.2004.01.037
20. Gorai, S.; Chaudhuri, S. Sonochemical synthesis and characterization of cage-like β-indium sulphide powder. *Mater. Chem. Phys.* **2005**, *89*, 332 – 335. https://doi.org/10.1016/j.matchemphys.2004.09.009
21. Raju, N. P.; Tripathi, D.; Lahiri, S.; Thangavel, R. Heat reflux sonochemical synthesis of Cu_3BiS_3 quantum dots: Experimental and first-principles investigation of spin-orbit coupling on structural, electronic, and optical properties. Sol Energy **2023**, *259*, 107-118. https://doi.org/10.1016/j.solener.2023.05.015

22. Pejova, B.; Sherif, E.; Minde, M. W. Sonochemically Synthesized Quantum Nanocrystals of Cubic $CuInS_2$: Evidence for Multifractal Surface Morphology, Size-Dependent Structure, and Particle Size Distribution. *J. Phys. Chem. C* **2020**, *124*, 20240-20255. https://doi.org/10.1021/acs.jpcc.0c06070
23. Pollet, B. G. The use of ultrasound for the fabrication of fuel cell materials. *Int J Hydrogen Energy* **2010**, *35*, 11986-12004. https://doi.org/10.1016/j.ijhydene.2010.08.021
24. Islam, M. H.; Paul, M. T. Y.; Burheim, O. S.; Pollet, B. G. Recent developments in the sonoelectrochemical synthesis of nanomaterials. *Ultrason. Sonochem.* **2019**, *59*, 104711. https://doi.org/10.1016/j.ultsonch.2019.104711
25. Ahmadi, S.; Mesbah, M.; Igwegbe, C. A.; Ezeliora, C. D.; Osagie, C.; Khan, N. A.; Dotto, G. L.; Salari, M.; Dehghani, M. H. Sono electro-chemical synthesis of $LaFeO_3$ nanoparticles for the removal of fluoride: Optimization and modeling using RSM, ANN and GA tools. *J. Environ. Chem. Eng.* **2021**, *9*, 105320. https://doi.org/10.1016/j.jece.2021.105320
26. Matyszczak, G.; Jóźwik, P.; Polesiak, E.; Sobieska, M.; Krawczyk, K.; Jastrzębski, C.; Płociński, T. Sonochemical preparation of SnS and SnS_2 nano- and micropowders and their characterization. *Ultrason. Sonochem.* **2021**, *75*, 105594. https://doi.org/10.1016/j.ultsonch.2021.105594
27. Jamali-Sheini, F.; Yousefi, R.; Bakr, N. A.; Cheraghizade, M.; Sookhakian, M.; Huang, N. M. Highly efficient photo-degradation of methyl blue and band gap shift of SnS nanoparticles under different sonication frequencies. *Materials Science in Semiconductor Processing* **2015**, *32*, 172-178
28. Cheraghizade, M.; Jamali-Sheini, F.; Yousefi, R.; Niknia, F.; Mahmoudian, M. R.; Sookhakian. M. The effect of tin sulfide quantum dots size on photocatalytic and photovoltaic performance. *Materials Chemistry and Physics* **2017**, *195*, 187-194
29. Jamali-Sheini, F.; Cheraghizade, M.; Yousefi, R. Ultrasonic synthesis of In-doped SnS nanoparticles and their physical properties. *Solid State Sciences* **2018**, *79*, 30-37.
30. Sakthi, P.; Uma, J.; Siva, C.; Balraj, B. Sonochemical synthesis of interconnected SnS nanocrystals for supercapacitor and solar-physical conversion applications. *Optical Materials* **2022**, *132*, 112759
31. García-Gómez, N. A.; de la Parra-Arcieniega,S. M.; Garza-Tovar, L. L.; Torres-González, L. C.; Sánchez, E. M. Ionic liquid-assisted sonochemical synthesis of SnS nanostructures. *Journal of Alloys and Compounds* **2014**, *588*, 638-643
32. Park, J.; Hwang, Ch. H.; Lee, W. Y.; Kim, Y.; Kim, H.; Shim, I.-W. Preparation of size-tunable SnS nanoparticles by a sonochemical method under multibubble sonoluminescence conditions. *Materials Letters* **2014**, *117*, 188-191.
33. Khimani, A. J.; Chaki, S. H.; Chauhan, S. M.; Mangrola, A. V.; Meena, R. R.; Deshpande, M. P. Synthesis, characterization, antimicrobial and antioxidant study of the facile sonochemically synthesized SnS_2 nanoparticles. *Nano-Structures & Nano-Objects* **2019**, *18*, 100286.
34. Khimani, A. J.; Chaki, S. H.; Giri, R. Kr.; Meena, R. R.; Kannaujiya, R. M.; Deshpande, M. P. Thermal exploration of sonochemically achieved SnS_2 nanoparticles: Elemental, structural, and morphological investigations of TG residual SnS_2. *Chemical Thermodynamics and Thermal Analysis* **2023**, *9*, 100104.
35. Mukaibo, H.; Yoshizawa, A.; Momma, T.; Osaka, T. Particle size and performance of SnS_2 anodes for rechargeable lithium batteries. *Journal of Power Sources* **2003**, *119-121*, 60-63.
36. Matyszczak, G.; Plocinski, T.; Dluzewski, P.; Fidler, A.; Jastrzebski, C.; Lawniczak-Jablonska, K.; Drzewiecka-Antonik, A.; Wolska, A.; Krawczyk, K. Sonochemical synthesis of SnS and SnS_2 quantum dots from aqueous solutions, and their photo- and sonocatalytic activity. *Ultrason. Sonochem.* **2024**, *105*, 106834.
37. Mead, D. G.; Irwin, J. C. Raman spectra of SnS_2 and $SnSe_2$. *Solid State Commun.* **1976**, *20*, 885-887. https://doi.org/10.1016/0038-1098(76)91297-7
38. Bialoglowski, M.; Jastrzebski, C.; Podsiadlo, S.; Jastrzebski, D. J.; Gajda, R.; Gebicki, W.; Wrzosek, P. A.; Wozniak, K. Synthesis of tin disulfide single crystals for nano-layer exfoliation. *Cryst. Res. Technol.* **2015**, *50*, 695-699. https://doi.org/10.1002/crat.201400436
39. Huang, Y.; Sutter, E.; Sadowski, J. T.; Cotlet, M.; Monti, O. L. A.; Racke, D. A.; Neupane, M. R.; Wickramaratne, D.; Lake, R. K.; Parkinson, B. A.; Sutter, P. Tin Disulfide-An Emerging Layered Metal Dichalcogenide Semiconductor: Materials Properties and Device Characteristics. *ACS Nano* **2014**, *8*, 10743-10755. https://doi.org/10.1021/nn504481r
40. Gao, Y.; Yin, P. Origin of asymmetric broadening of Raman peak profiles in Si nanocrystals. *Sci. Rep.* **2017**, *7*, 43602. https://doi.org/10.1038/srep43602
41. Julien, C.; Mavi, H. S.; Jain, K. P.; Balkanski, M.; Perez-Vicente, C.; Morales, J. Resonant raman scattering studies of SnS_2 crystals. *Materials Science and Engineering: B* **1994**, *23*, 98-104. https://doi.org/10.1016/0921-5107(94)90341-7
42. Burton, L. A.; Whittles, T. J.; Hesp, D.; Linhart, W. M.; Skelton, J. M.; Hou, B.; Webster, R. F.; O'Dowd, G.; Reece, C.; Cherns, D.; Fermin, D. J.; Veal, T. D.; Dhanak, V. R.; Walsh, A. Electronic and optical properties of single crystal SnS_2: an earth-abundant disulfide photocatalyst. *J. Mater. Chem. A* **2016**, *4*, 1312-1318. https://doi.org/10.1039/C5TA08214E

 doi:10.20944/preprints202411.1987.v1

43. Schockley, W.; Queisser, H. J. Detailed Balance Limit of Efficiency of p-n Junction Solar Cells. *J. Appl. Phys.* **1961**, *32*, 510-519.